SOVIET PHYSICS USPEKHI VOLUME 11, NUMBER 2 SEPTEMBER-OCTOBER 1968

539.124.6

ANNIHILATION OF POSITRONS IN METALS

V. L. SEDOV

Moscow State University

Usp. Fiz. Nauk 94, 417–438 (March, 1968)

A large number of experimental and theoretical papers devoted to annihilation of positrons in solids have been published by now. Initially, in most cases, the effects connected with positron–electron annihilation in matter were studied "for their own sake." However, as experimental and theoretical results in this field were accumulated, and also as the research procedures became more refined, it became possible to use effects connected with annihilation for the study of the properties of solids. By way of an example, we can refer to investigations in which the positrons were used to study the topology of Fermi surfaces and the magnetic structures of ferromagnets (Ch. III and V).

In experiments on annihilation, it is customary to use as positron sources radioactive isotopes that emit positrons as a result of β^+ decay. The positrons produced in this case have an appreciable kinetic energy, on the order of 1 MeV. After entering the substance, the positrons lose their kinetic energy by collision with the electrons, and enter into equilibrium with the surrounding medium (they become "thermalizes"). It is important that the thermalization time ($\sim 10^{-12}$ sec[1]) is much shorter than the lifetime of the positron with respect to annihilation (10^{-10} sec).

Another important circumstance is that the thermalized positron, owing to the Coulomb repulsion by the nucleus, cannot penetrate inside the ionic core. This means that the positrons annihilate essentially only with valence electrons.

Thus, the properties of the annihilation radiation are connected, by the different laws governing the conservation of the physical quantities, only with the properties of the valence electrons and the thermalized positrons.

Let us list the main effects discussed in the present article.

1. Positron lifetime in a metal. This quantity is determined by the density of the valence electrons and by the mechanism of the interaction between the positron and the electronic medium surrounding it (Ch. II). Experiments on the determination of the lifetime can lead to conclusions on the formation of bound electron–positron states (Ch. I).

2. Distribution of the pairs of γ quanta produced as a result of two-quantum annihilation with respect to the momenta (angular correlation of the annihilation quanta). This effect yields information on the distribution of the valence electrons in momentum space, and, in particular, makes it possible to study the topology of the Fermi surface (Ch. III). The angular-correlation effect can also yield data on the "effective masses" of positrons in metals (Ch. IV).

3. In the annihilation of polarized positrons in ferromagnetic metals, the mutual orientation of the vectors of sample magnetization and positron polarization influences the properties of the annihilation radiation (Ch. V). These effects yield information on the spin polarization of different valence electrons of the groups of ferromagnetic metals.

4. In the annihilation of positrons in condensed media, the ratio of the cases of annihilation in which different numbers of γ are produced may be different than for an isolated electron–positron pair. The corresponding results, obtained in the annihilation of positrons in metals, are considered in Ch. VI.

I. THE QUESTION OF THE POSSIBLE EXISTENCE OF POSITRONIUM IN METALS

An isolated electron–positron pair can produce a bound state—a positronium atom. If we disregard relativistic effects, then the quantum-mechanical description of the properties of positronium becomes similar to a description of the properties of the hydrogen atom.[17]

Indeed, the Schrödinger equation for the electron–positron pair is

$$\left[\frac{1}{2m}(\hat{p}_e^2+\hat{p}_p^2)-\frac{e^2}{|\mathbf{x}_e-\mathbf{x}_p|}\right]\Psi(\mathbf{x}_e,\ \mathbf{x}_p)=E\Psi(\mathbf{x}_e,\ \mathbf{x}_p). \qquad (1.1)$$

In a coordinate frame in which the mass center of the particle pair in question is at rest, this equation can be rewritten as follows

$$\left(\frac{1}{2m}\hat{p}^2-\frac{e^2}{|\mathbf{x}|}\right)\Phi(\mathbf{x})=E\Phi(\mathbf{x}), \qquad (1.2)$$

where $\mathbf{x} = \mathbf{x}_e - \mathbf{x}_p$ and $\mathbf{p} = \mathbf{p}_e = -\mathbf{p}_p$.

Equation (1.2) coincides with the equation for the hydrogen atom, if we replace in the latter the electron mass m by m/2. Such a substitution does not disturb the qualitative analogy between the properties of positronium and the hydrogen atom. The quantitative difference, on the other hand, lies in the fact that the values of the energy levels of the positronium are half as large as the corresponding levels of the hydrogen atom, and the radii of the orbits are twice as large.

For real metals, the average distances between the valence electrons are of the same order as the radius of the positronium orbit in vacuum. It is therefore unclear a priori whether electron–positron bound states can exist in metals. No rigorous solution of this problem has been found as yet. Qualitative considerations with respect to this fact were advanced by Ferrell,[3] and also by Karpman and Fisher.[2]

More definite results were obtained in [4, 5], where this question was investigated on the basis of the single-electron approximation, without any account of the periodic potential of the lattice. The role of the surrounding electron medium was taken into account in the following manner: 1) A limitation that follows from the Pauli principle was imposed on the wave function of the particle pair in question; namely, if $\Phi(\mathbf{p}_e, \mathbf{p}_p)$ is the

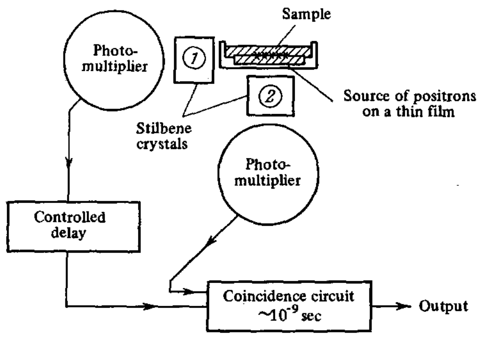

FIG. 1. Schematic diagram of setup used by Bell and Graham [8] to measure the lifetime of positrons in condensed substances.

wave function in the momentum representation, describing the bound state of the electron-positron pair, then $\Phi(p_e, p_p) = 0$ when $|p_e| < p_F$ (p_F—end-point momentum); 2) the Coulomb potential of the interaction of the particles under consideration was replaced by the screened static potential. An investigation of this question with the aid of a variational method has led Held and Kahana[4] to the conclusion that a stable formation ("quasipositronium") is possible only when $r_s \geq 8.6$.* There is no doubt that the calculations performed in this manner are based on rather crude simplifications, so that the problem of determining the limiting electron-gas concentration necessary for the formation of quasipositronium cannot be regarded as finally solved.

The experimental data on the whole also indicate that positronium is not formed in metals. The corresponding experiments will be considered in Chs. II and III.

II. LIFETIMES OF POSITRONS IN METALS

The experimental investigations of the lifetimes of positrons in different metals were reported in [6-15]. The simplest setup for the measurement of the positron lifetime in a solid is shown in Fig. 1.[8] In this case the positron source, radioactive Na^{22}, is located directly inside the investigated sample. The instant of production of the positron is determined by registration of the 1.28-MeV γ quantum (counter 1) that accompanies the β decay of the Na^{22} nuclei. The instant of annihilation is determined by the appearance of annihilation quanta with energy 0.511 MeV (counter 2).

Figure 2 shows the experimental curves obtained by Bell and Jorgensen[12] by this method for aluminum and cesium. The ordinate axis represents the logarithms of the number of coincidences of the signals from counters 1 and 2 per unit time; the abscissas represent the delay time of the signals from counter 2 relative to the signals from counter 1. The tangents to the right parts of the curves shown in Fig. 2 determine the sought value of τ. Attention is called to the existence of a second lifetime component τ' for the aluminum. According to [10-12], the second lifetime component was observed for Al, Li, Na, and Cu. In all cases the intensity of τ' is much smaller than the intensity of the main component of the lifetime τ. According to [12], the number of positrons annihilating with a time τ' does not exceed 6.5% of the total number.

*r_s—radius of unit electron sphere, expressed in units of the Bohr-orbit radius. For real metals $1.8 \lesssim r_s \lesssim 5.5$.

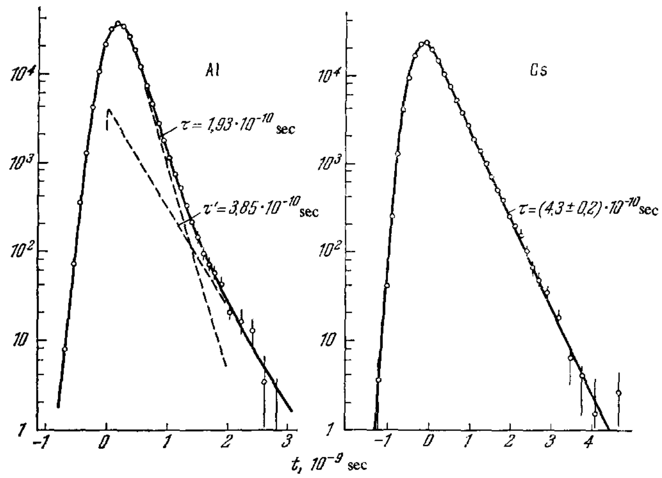

FIG. 2. Delayed-coincidence curves characterizing the lifetime of positrons in aluminum and cesium [12] (ordinates—coincidence counting rate).

It is known from earlier investigations (e.g., [16]) that the presence of two lifetime components for positrons in annihilation in gases is connected with the formation of para- and orthopositronium (the states ^1S and ^3S; $\tau_1 = 1.25 \times 10^{-10}$ sec, $\tau_2 = 1.41 \times 10^{-7}$ sec). The difference between τ_1 and τ_2 is due in this case to the fact that the annihilation of the electron-positron pair from the two states ^1S and ^3S proceeds in different fashion. As a result of charge-parity conservation, the states ^1S and ^3S can decay only into even and odd numbers of γ quanta, respectively (see, e.g., [17]).

It is firmly established by now that positronium can be produced in certain dielectrics (see, e.g., [16, 79]). In this case there is also observed an intense long-lived component, but its duration is much shorter than the value of τ_2 for the free ortho-positronium. This circumstance is connected with the possibility that a positron in a bound ^3S state may capture an electron from the surrounding medium with a suitable spin direction (for two-quantum annihilation) (pick-off effect).

The causes of the appearance of the weak component τ' in the case of certain metals are presently unknown. There is an indication[11] that the intensity of τ' depends on the quality of the samples. It would be natural to assume in this connection that the second component of the positron lifetime in metals is the result of the formation of bound electron-positron states near lattice defects.

In order to explain the values of τ observed for metals, it is necessary to take into account the interaction of the positron with the electron medium surrounding it. Ferrell[3] proposed that the effects due to this interaction are fully determined by the electron density at the point of the positron location. According to this assumption, the annihilation probability W (the reciprocal of the lifetime) is proportional to the electron density at the location of the positron, averaged over all the possible positron locations. This definition means that

$$W = C \int \langle 0 | (\psi^+(\mathbf{x})\, \psi(\mathbf{x}))\, (\varphi^+(\mathbf{x})\, \varphi(\mathbf{x})) | 0 \rangle\, d^3\mathbf{x}, \qquad (2.1)$$

where $\psi(\mathbf{x})$ and $\varphi(\mathbf{x})$ are the operators of second quantization of the electron and positron fields in the Schrödinger representation. The spin indices have been omitted for simplicity. According to [3], the constant C can be determined from the relation

$$C = \frac{1}{4}\frac{W_{\rm pos}}{|\Phi(0)|^2}. \qquad (2.2)$$

Here $W_{\rm pos}$ is the probability of para-positronium annihilation and $\Phi(\mathbf{r})$ is the para-positronium wave function. The factor $\frac{1}{4}$ is the result of averaging over the spins of the particles that annihilate in the metal.

In concrete calculations of W it is convenient to use the two-particle electron–positron Green's function[13]

$$G_{ep}(x,\ y;\ x',\ y') = \langle 0\,|T\widetilde{\psi}(x)\,\widetilde{\varphi}(y)\,\widetilde{\psi}^{+}(x')\,\widetilde{\varphi}^{+}(y')\,|\,0\rangle; \qquad (2.3)$$

T is the chronological ordering symbol and $\widetilde{\psi}(x)$ and $\widetilde{\varphi}(y)$ are the operators of the second quantization of the electron and positron fields in the Heisenberg representation.

It follows from (2.1) and (2.3) that

$$W = -C\lim_{t'\to t+0}\int G_{ep}(\mathbf{x}t,\ \mathbf{x}t;\ \mathbf{x}t',\ \mathbf{x}t')\,d^3\mathbf{x}. \qquad (2.4)$$

This expression can be represented in a more lucid form by using the well known integral relation for the two-particle Green's function (see, e.g., [81]), which for this case is of the form

$$G_{ep}(x,\ y;\ x',\ y') = G_e(x-x')\,G_p(y-y')$$
$$+\,i\int G_e(x-x_1)\,G_p(y-y_1)\,\Gamma(x_1,\ y_1;\ x_2,\ y_2)\,G_e(x_2-x')\,G_p(y_2-y')\,d^4x_1 d^4y_1\,d^4x_2\,d^4y_2. \qquad (2.5)$$

Here $G_e(x-x')$ and $G_p(y-y')$ are the single-particle electron and positron Green's functions, and $\Gamma(x_1, y_1; x_2, y_2)$ is the vertex part.

The individual terms arising when (2.5) is substituted in (2.4) have the following physical meaning. The first term, which contains only the product of two single-particle Green's functions, determines the probability of annihilation without allowance for the polarization of the electron gas by the positron. The second term, which contains the vertex part, takes into account the contribution to the annihilation probability from increase of the electron density at the positron location point. The magnitude of this contribution, for the electron-gas concentration corresponding to the case of aluminum, is illustrated by the data given in the table.

Attention should be called to the fact that expression (2.1), in general, does not take into account all the possible annihilation channels. For example, this expression does not allow for the possibility of positron annihilation with one of the electrons surrounding it, and simultaneous production of additional electron–hole excitations in the system. The probability of positron annihilation with simultaneous production of one electron–hole pair was estimated in [22]. At an electron-gas density corresponding to real metals, the probability of this effect is a quantity of the same order (10^9 sec^{-1}) as the probability of ordinary two-quantum annihilation.

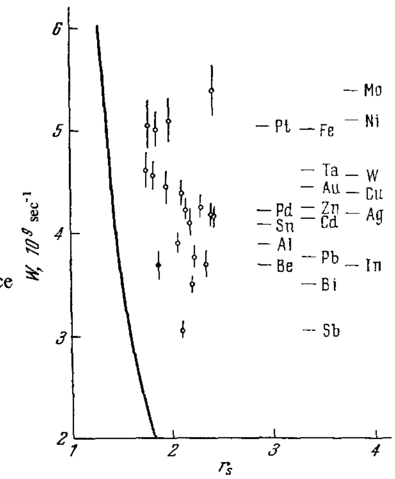

FIG. 3. Experimental values of the annihilation probability W for different metals vs. the values of r_s proposed for them [13]. The solid line corresponds to the dependence of W on r_s in the case of an ideal electron gas.

A metal model in ħ which the valence electrons are regarded as a homogeneous gas, without allowance for the ion lattice, cannot pretend to agree in detail with the results of positron-annihilation experiments. Figure 3 shows the experimental values[13] of W for different metals as a function of the values of r_s proposed for them. It is significant that the experimental points do not fall in this case on a smooth curve.

Measurements of the lifetime of positrons in rare-earth metals, performed by Rodda and Stewart,[15] have shown that for trivalent elements of this group the value of W varies little in the entire series of these elements as the 4f shell is filled. The average lifetime for these elements, according to [15], is $\tau_{\rm Al} + 0.675\times10^{-10}$ sec. The average deviation from this value is $\pm0.035\times10^{-10}$ sec. Starting from this result, the authors of [15] have concluded that the positrons do not annihilate in a noticeable number of cases with the 4f electrons of the rare-earth elements. Gustafson and Mackintosh,[48] investigating the effect of angular correlation of the annihilation quanta for rare-earth metals, concluded that the results of Rodda and Stewart must be attributed to

Probability of positron annihilation in aluminum

Method of determination	W, 10^9 sec^{-1}	Literature
Experiment	5.3±0.6 3.9±0.1 4.5±0.2	12 13 15
Calculation		
a) Without allowance for the interaction of the positron with the surrounding medium	1.35	
b) With allowance of the increase of the electron density at the point of positron location, but without allowance of the emission of additional electron-hole pairs (in the approximation of a condensed electron gas)	3.3	18
c) With allowance of only those cases of annihilation at which emission of an electron-hole pair takes place (this quantity is only part of the total annihilation probability)	3.1	22

"mutual cancellation" of two effects. The increase of the number of 4f electrons gives a positive contribution to the annihilation probability. At the same time, the increase of the nuclear charge leads to a decrease of the overlap of the wave functions of the 5s and 5p shells with the wave function of the positron, thus compensating for the increase of W as a result of the increase of the number of 4f electrons.

III. ANGULAR CORRELATION OF THE ANNIHILATION γ QUANTA

1. Main Properties of the Angular-correlation Effect

The energy and momentum conservation laws in the annihilation of an electron positron pair lead to definite relations between the direction of propagation of the annihilation quanta and their frequency. In the case of interest to us, the main contribution to the energy of the particles is made by their rest masses. This means that the energy of each of the two γ quanta differs little from mc^2, and the angle between their propagation direction is close to 180°.

Let $p_\perp$ and $p_\parallel$ be the components of the c.m.s. momentum of the annihilating pair perpendicular and parallel, respectively, to the direction of emission of γ quanta with momenta $\mathbf{k}_1$ and $\mathbf{k}_2$ (Fig. 4). It is obvious that when $|\mathbf{p}_\perp + \mathbf{p}_\parallel| \ll mc$ the angle θ is determined by the relation

$$\sin\theta \simeq \frac{p_\perp}{mc}. \tag{3.1}$$

At values of $p_\perp$ corresponding to the characteristic values of the Fermi momenta of metals, we have $\theta \sim (5-10)\times 10^{-3}$ rad. The difference between the frequency of photons with momenta k_1 and k_2 (Doppler shift) is given in this case by the expression

$$\Delta\omega = \frac{p_\parallel c}{\hbar}. \tag{3.2}$$

Observation of this effect entails great experimental difficulties.[23] At the present time, the Doppler shift of the frequencies of the annihilation quanta is not used to study the properties of solids.

The experimental setup for the observation of the angular correlation of the annihilation quanta is shown in Fig. 5.[30] Signals from the photomultipliers of this setup are fed to a coincidence circuit. An investigation of the distribution of the γ-quanta pair with respect to θ is carried out by measuring the counting rate of the counter signals that coincide in time, as a function of the angle of rotation of the right-hand counter relative to the sample. Since this distribution lies actually within a narrow angle interval ($\theta_F \ll \pi$), it can be assumed that a γ-quantum pair deflected by an angle θ has a z-component of momentum $p_z = mc\theta$.

A study of the effect of the angular correlation is

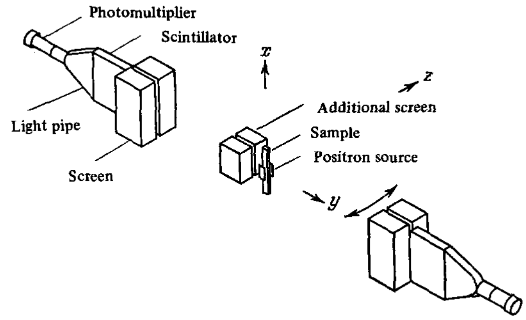

FIG. 5. Experimental setup used by Lang and De Benedetti [30] to investigate the angular correlation of the annihilation radiation in different substances.

usually aimed at obtaining information on the electron distribution function in momentum space. If we disregard effects due to the interaction between the positron and electrons or ions, then we get for the experimentally determined function N $\theta = p_z/mc$) the following expression:

$$N(\theta) = A \int_{-\infty}^{\infty}\int_{-\infty}^{\infty} n(p_x, p_y, p_z)\, dp_x\, dp_y. \tag{3.3}$$

Here $n(p_x, p_y, p_z)$ is the electron momentum distribution function. The values of the constant A are determined by the parameters of the setup.

It is easy to show that for an ideal degenerate Fermi gas the value of $N(\theta)$ is proportional to $p_F^2 - p_z^2$. Indeed, in this approximation the function $n(p_x, p_y, p_z)$ is equal to unity inside the Fermi sphere and to zero outside. Therefore the integral in (3.3) represents in this case the area of the circle produced when the Fermi sphere is intersected by a plane perpendicular to the z axis and located a distance p_z from the center of the sphere (Fig. 6). Thus, in the present approximation $N(\theta)$ is an inverted parabola whose intercepts with the horizontal axis determine the end-point momentum.

The effect of the angular correlation of annihilation quanta was investigated experimentally for metals in [24-52]. Figure 7 shows the results of measurements made by Stewart.[32]

It is of interest to compare the experimental curves for different metals with parabolas corresponding to ideal electron gases. The results of such comparisons, taken from [28], are shown in Fig. 8. The central parts of the solid curves are described by parabolas calculated for the given metals, of the form $p_F^2 - p_z^2$. The horizontal coordinates of the kinks correspond to the calculated values of p_F. Thus, the curves shown in Fig. 8 can be regarded, with a certain degree of approximation, as consisting of two parts: parabolas and "tails." The appearance of the "tails" is due to the following physical causes:

1. The states of the valence electrons (in the single-

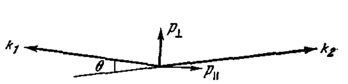

FIG. 4. The component $p_\perp$ of the c.m.s. momentum of the annihilating pair deflects the photon propagation directions k_1 and k_2 from their mutually-opposite direction by an angle θ.

FIG. 6. In the case of an ideal gas the number of γ-quantum pairs registered per unit time with the aid of the setup shown in Fig. 5, for a given value of the angle θ ($\theta = p_c/mc$), is proportional to the shaded area, i.e., to the quantity $p_F^2 - p_F^2$.

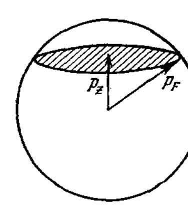

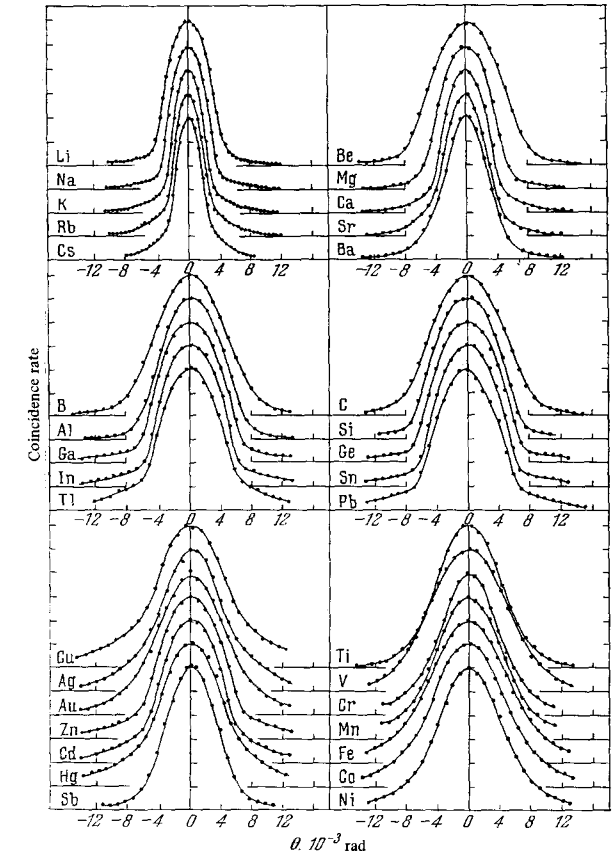

FIG. 7. Plots of angular correlations of annihilation γ quanta for different elements, obtained by Stewart [32].

electron approximation) do not correspond to definite values of the momentum, owing to interaction between the electrons and the ion lattice.

In order to describe the role of this factor, let us consider the annihilation of an electron whose state is described by a Bloch wave function $u_k(r)\exp(i\mathbf{k}\cdot\mathbf{r})$ and a thermalized electron with a wave function $\Psi_{0,p}(r)$. According to Ferrell (see Ch. II), the probability of annihilation with emission of γ quanta having a total momentum **p** is proportional to the probability of observing the electron-positron pair under consideration simultaneously in one and the same point of space with

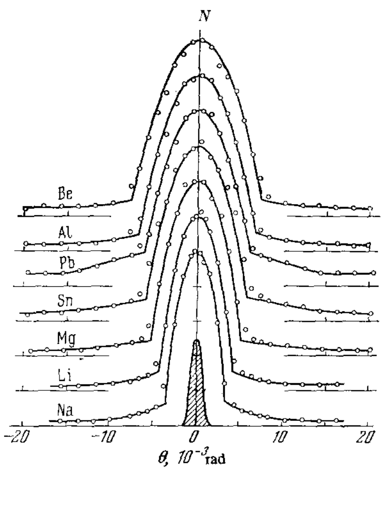

FIG. 8. Comparison of experimental results for the effect of the angular correlation in different metals with the parabolas describing the momentum distribution of the electrons in these metals, without allowance for any types of interaction. The lower ends of the parabolas (the kink points) correspond to the values of the end-point momenta calculated for the given metals. The shaded area shows the angular resolution of the apparatus [28].

the same value of the total momentum. The latter quantity, as follows from the well known quantum-mechanical rules, is given by the expression

$$\rho_{\mathbf{k}}(\mathbf{p})=\frac{1}{V^2}\left|\int u_{\mathbf{k}}(\mathbf{r})\,\Psi_{0,\,p}(\mathbf{r})\exp\left[i\left(\mathbf{k}-\mathbf{p}\right)\mathbf{r}\right]dV\right|^2; \qquad (3.4)$$

V is the volume of the system under consideration.

In order to obtain the total probability of positron annihilation with emission of photons having a total momentum **p**, it is necessary to sum $\rho_k(\mathbf{p})$ over all **k** corresponding to the occupied states.

It is seen from (3.4) that the stronger the localization of the electrons participating in the annihilation near the ionic core, the more "smeared" is the observed picture of the angular correlation of the γ quanta. This effect plays an important role in the annihilation of positrons in transition metals. The angular-correlation curves for these metals have a strongly "smeared" form (see Fig. 7) owing to the annihilation of the positrons with electrons from the internal unfilled shells.

2. The interaction between the positrons and the ions of the crystal lattice determines the concrete form of the positron wave function $\Psi_{0,p}(\mathbf{r})$ and thus, in accordance with (3.4), influences the value of $\rho_k(\mathbf{p})$.

When account is taken of the interaction between the positrons and the lattice, one frequently makes use of an approximation in which it is assumed that the positron distribution density is constant between lattice points and is equal to zero inside the core.[35] Within the framework of such a model, we arrive at the effect called the "excluded volume effect."

3. The cause of the deviation of the experimental curves from the simple parabolic dependence is the ion and electron-electron interaction in the electron gas.

If we disregard the possible appearance of additional electron-hole pairs in the annihilation, then the influence of the electron-electron interaction on the angular correlation can be taken into account with the aid of the two-particle electron-positron Green's function.[54] In this case the probability of production of two γ quanta with total momentum **p** is given by

$$W(\mathbf{p})=-\lambda\lim_{t'\to t+0}\int\exp\left[-i\mathbf{p}(\mathbf{x}-\mathbf{x}')\right]G_{ep}(\mathbf{x}t,\ \mathbf{x}t;\ \mathbf{x}'t',\ \mathbf{x}'t')\,d^3\mathbf{x}\,d^3\mathbf{x}', \qquad (3.5)$$

where $\lambda = C/(2\pi)^3$ and the constant C is given by (2.2).

If we substitute in (3.5) the expression for the two-particle electron-positron Green's function (2.5) and express $G_e(x-x')G_p(x-x')$ in the form $G_e(x-x') \times [G_p^0(x-x') + \delta G_p(x-x')]$, then $W(\mathbf{p})$ turns out to be equal to the sum of three terms having the following physical meaning:

a) The term containing $G_e(x-x')G_p^0(x-x')$ determines the annihilation probability without account of the interaction between the annihilating particles, but with allowance for the real electron momentum distribution, namely:

$$W_1(\mathbf{p}) = \lambda n(\mathbf{p}), \qquad (3.6)$$

where $n(\mathbf{p})$ is the momentum distribution for the real electron gas.

b) The term containing the factor $G_e(x-x') \times \delta G_p(x-x')$ describes the interaction of the positron with the surrounding electron medium (the self-energy effects of the positron).

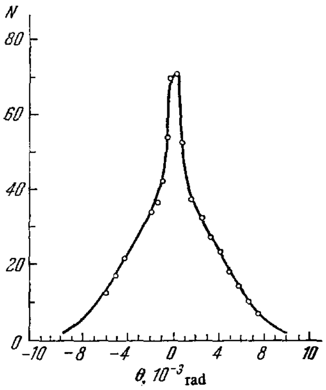

FIG. 9. Angular correlation of the annihilation radiation for ice at −40°C [50]. The peak at small angles θ (the "narrow" component) indicates the existence of positronium.

c) The last term containing the vertex part takes into account the interaction of the annihilating particles.

A detailed investigation of W(p) with the aid of expression (3.5) was made by Carbotte and Kahana.[54]

From the investigations of the angular-correlation effects it is possible to deduce the presence of positronium in the investigated substances. For dielectrics in which positronium is produced (according to data based on lifetime measurements), the angular-correlation curves have at the origin the so-called "narrow component." Figure 9 shows the curve for ice, which has the indicated singularity. The appearance of the "narrow component" is connected with the fact that the positronium is thermalized in the substance. No "narrow component" was observed in metals. This is one of the proofs of the absence of positronium in metals.

2. Investigations of the Fermi Surface of Metals with the Aid of the Effect of Angular Correlation of Annihilation Quanta

One of the interesting possibilities of using the effect of angular correlation of the annihilation quanta is to employ this effect to study the Fermi surfaces of metals. It is important that this method does not require the use of low temperatures or strong magnetic fields, and does not impose too stringent requirements on the purity of the investigated samples. The main difficulty encountered in the interpretation of the experimental results on the angular correlation of the annihilation quanta is that, as follows from (3.4), the observed picture of the momentum distribution of the γ-quantum pairs depends on the concrete form of the wave functions of the electron and the positron. In this connection, there is presently no universal method for uniquely determining the topology of Fermi surfaces on the basis of experimental data on the angular correlation of the annihilation radiation. Attempts to investigate the Fermi surface of metals with the aid of positrons were made in [35, 38, 41, 42, 44].

The greatest success, from the methodological point of view, was attained by Fujiwara and Sueoka,[44] who used for the investigation a copper single crystal irradiated beforehand by neutrons, in order to form in it a certain amount of the β^+-radioactive isotope Cu^{64}. Thus, in this case the source of positrons of appreciable activity (1–2 Curie) was located in the sample itself. This circumstance has enabled Fujiwara and Sueoka to greatly improve the geometry of the setup. Figure 10 shows two different setups for the measurements of the angular correlation of annihilation radiation. The upper setup shows the usual variant of the setup for the measurement of the distribution of γ-quantum pairs with respect to a specified momentum projection on a specified direction at arbitrary values of two other momentum components. In the lower half of Fig. 10 is shown the experimental setup used by Fujiwara and Sueoka. Such a setup makes it possible to study in greater detail the momentum distribution of the electrons in the metal, since one of the momentum components (in this case, the vertical component) is fixed.

Figure 11 shows the angular-correlation plots obtained by these authors at different sample orientations. The suitably oriented Fermi surfaces of copper are shown over the curves. Curve a) corresponds to a sample orientation in which the direction of the emission of the annihilation radiation is parallel to [111], and the momentum distribution was plotted relative to the [$\bar{1}$10] direction. For curve b), the direction of the radiation is parallel to [1$\bar{1}$0], and the momentum distribution was

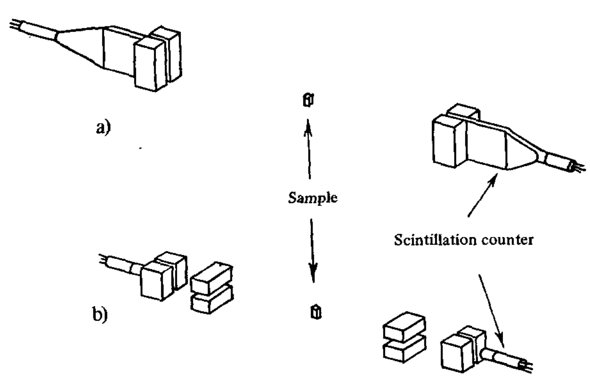

FIG. 10. Two setups for the investigation of the effect of the angular correlation of annihilation quanta. Scheme (b) makes it possible to investigate this effect at a fixed value of the vertical projection of the momentum.

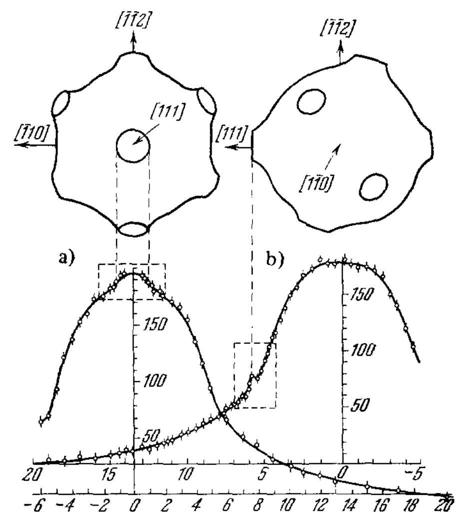

FIG. 11. Angular-correlation plots obtained by Fujiwara and Sueoka [44] for single-crystal copper with the aid of the setup of Fig. 10b. The Fermi surface of copper is shown over the curves in two positions corresponding to different orientations of the sample (the abscissas represent θ in units of 10^{-3} rad).

investigated with respect to [111]. The dashed lines in Fig. 11 border the angular-correlation-curve sections that are connected with the existence of "projections" on the Fermi surface of copper in directions such as [111] and tangent to the zone boundaries. The authors determined the radius of the circle produced by the contact between the "projection" and the plane that serves the zone boundary. According to this paper, this quantity is equal to 2.7×10^{-20} g-cm-sec^{-1}, which agrees with earlier investigations of the Fermi surface of copper by other methods.

Let us examine, following [33], the influence exerted on the angular-correlation effect by the orientation of the Fermi surface relative to the zone boundaries. If we neglect the electron–electron and electron–positron interactions, then the momentum distribution of the γ-quantum pairs will be proportional to m(p):

$$m(\mathbf{p}) = \sum_{\mathbf{k}}{}' \rho_{\mathbf{k}}(\mathbf{p}). \tag{3.7}$$

The function $\rho_{\mathbf{k}}(\mathbf{p})$ is determined by (3.4). The prime at the summation sign denotes that the summation is carried out only over the occupied electron states.

The quantity $u_{\mathbf{k}}(\mathbf{r})\Psi_{0,\mathbf{p}}(\mathbf{r})$ is a periodic function of $\mathbf{r}$, and therefore

$$u_{\mathbf{k}}(\mathbf{r})\Psi_{0,\,\mathbf{p}}(\mathbf{r}) = \sum_{\boldsymbol{\tau}} A(\mathbf{k},\ \boldsymbol{\tau}) \exp(i\boldsymbol{\tau}\mathbf{r}). \tag{3.8}$$

The sum is taken here over all the reciprocal-lattice vectors $\boldsymbol{\tau}$. Using (3.4), (3.7), and (3.8), we can easily get

$$m(\mathbf{p}) = \sum_{\boldsymbol{\tau}}{}' |A(\mathbf{p}-\boldsymbol{\tau},\ \boldsymbol{\tau})|^2. \tag{3.9}$$

In this expression, the summation is carried out over those values of $\boldsymbol{\tau}$, for which the vector $\mathbf{p} - \boldsymbol{\tau}$ lies inside the volume bounded by the Fermi surface. Thus, the expression for m(p) depends on the orientation of the Fermi surface relative to boundaries of the zone. Figures 12–14 show plots of the function m(p) near the zone boundary as functions of the momentum component p_n (which is normal to the given boundary plane), as calculated by Berko and Plaskett[33] in the approximation of "almost free electrons" for three cases: 1) the Fermi surface coincides with the zone boundary (Fig. 12); 2) the Fermi surface lies below the zone boundary (Fig. 13); 3) the first zone is completely filled, and the Fermi surface lies in the second zone (Fig. 14). In cases 2) and 3) the wave vectors of the Fermi surfaces differ from $\tau/2$ by an amount $\pm|V_\tau|/\tau$ (V_τ—Fourier component of the lattice potential).

IV. EFFECTIVE MASS OF POSITRON

When account is taken of the interaction with the medium surrounding it, a thermalized positron can be regarded as a quasiparticle. This circumstance makes it possible to assign formally to the positron a certain effective mass. The value of the effective mass of the positron depends on the following physical processes: 1) electron–positron interaction, 2) interaction of the positron and the periodic lattice potential (the band effective mass), 3) the interaction of the positron with the phonons.

Stewart and Shand[55] proposed to determine the effective mass of the positron from the temperature dependence of the function $N(\theta)$ at values of θ close to θ_F. At 0°K this function should have a discontinuity of

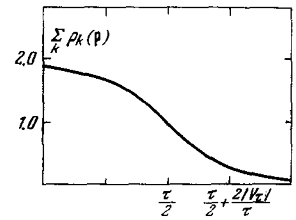

FIG. 12. Electron distribution with respect to the momenta p_n near the zone boundary ($\tau/2$), calculated in the "almost free electron" approximation. The Fermi surface coincides with the zone boundary [33].

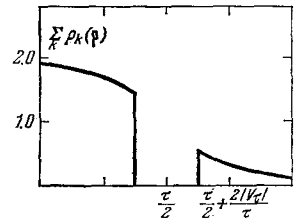

FIG. 13. Electron distribution with respect to the momenta p_n near the zone boundary ($\tau/2$), calculated in the "almost free electron" approximation. The Fermi surface lies below the zone boundary [33].

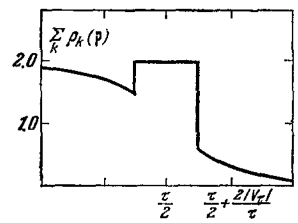

FIG. 14. Electron distribution with respect to the momenta p_n near the zone boundary ($\tau/2$), calculated in the "almost free electron" approximation. The Fermi surface located above the zone boundary [33].

the derivative at $\theta = \theta_F$ even when rigorous account is taken of all the interactions between the particles in question. With increasing temperature, this kink becomes smoothed out. Figure 15 shows the experimental plots of the angular correlations, obtained by Stewart and Shand for sodium at different temperatures. The curves show that the kink corresponding to the end-point momentum becomes smeared out with increasing temperature. This effect is produced by the following factors:

a) The temperature dependence of the electron mo-

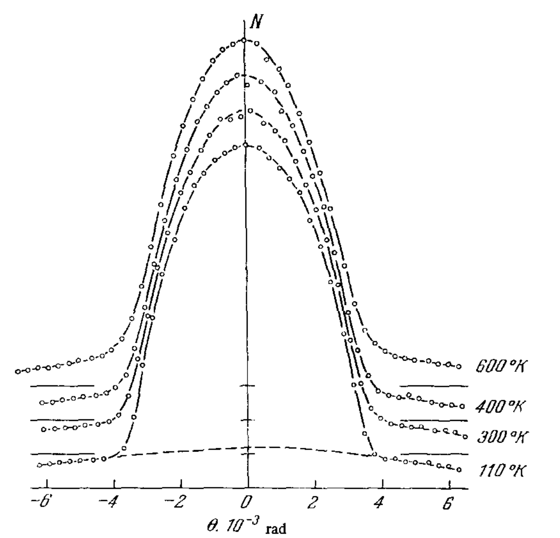

FIG. 15. Plots of the angular correlations of annihilation radiation for sodium at different temperatures [55]. These curves illustrate the smearing (with increasing temperature) of the kink corresponding to the end-point momentum.

mentum distribution. In the simplest case this effect is described by the Fermi–Dirac function

$$f_-(\mathbf{p}) = \frac{1}{\exp[(\varepsilon(\mathbf{p}) - \mu)/kT] + 1}. \tag{4.1}$$

b) Thermal motion of the positrons, described by the Maxwellian momentum distribution

$$g_+(\mathbf{p}) = \frac{1}{(2\pi m_+^* kT)^{3/2}} \exp[-\mathbf{p}^2/2m_+^* kT]. \tag{4.2}$$

c) Temperature dependence of the electron mean free path.

d) Thermal expansion of the sample.

The momentum distribution of the mass centers of the the annihilating particles, with allowance for the facts noted in items a) and b), is obviously given by the expression

$$F(\mathbf{p}) = \iint f_-(\mathbf{p}_1)\, g_+(\mathbf{p}_2)\, \delta(\mathbf{p} - \mathbf{p}_1 - \mathbf{p}_2)\, d^3\mathbf{p}_1\, d^3\mathbf{p}_2. \tag{4.3}$$

From this it follows directly that when only these two effects are taken into account we have

$$N(\theta = p_z/mc) = A \int f_-(\mathbf{p}_1)\, g_+(\mathbf{p} - \mathbf{p}_1)\, d^3\mathbf{p}_1\, dp_x\, dp_y, \tag{4.4}$$

where A is a proportionality constant.

It is convenient to measure in the experiment the temperature dependence of $N(\theta)$ at $\theta = \theta_F$. For this quantity, in the case of a spherical Fermi surface, it is possible to obtain, by starting from (4.4), the following relation:[57]

$$\frac{N(\theta_F)}{N(0)} = \frac{1}{\pi^{1/2}} \left(\frac{m_+^* T}{m_-^* T_F}\right)^{1/2} - \frac{1}{4} \frac{T}{T_F} \frac{m_+^*}{m_-^*} + O\left(\frac{T}{T_F}\right); \tag{4.5}$$

T_F—degeneracy temperature of the electron gas.

Inasmuch as under real conditions $T \ll T_F$, the principal role in (4.5) is played by the first term. In this approximation, it is possible to neglect the influence of the mean free path of the electrons and of the thermal expansion on $N(\theta_F)$, since, in accordance with [57], these factors lead to the appearance in (4.2) of additional terms proportional to T/T_F and to higher powers of this ratio. From the results of the experiment of Stewart and Shand[55] it follows that for sodium $m_+^* = (1.9 \pm 0.4)m$. Numerical calculations of the band part of the effective mass of the positron in sodium[56] have shown that this quantity is equal to 1.06m. The value of the effective mass of the positron, due only to the electron–positron interaction, was investigated theoretically by Hamann.[58] For sodium, this quantity turned out to be 1.18m.

V. ANNIHILATION OF POLARIZED POSITRONS IN FERROMAGNETIC METALS

The positron sources usually employed in experiments on annihilation are the radioactive isotopes Na^{22}, Co^{57}, Co^{58}, and Cu^{64}. The β decay of these isotopes gives rise to longitudinally-polarized positrons, the degree of polarization of which is equal to $\langle v/c \rangle$. Thermalization of the positrons in a solid does not change appreciably the value of their polarization.[80] Thus, a system consisting of polarized positrons and polarized electrons is realized in experiments on the annihilation of positrons in ferromagnetic metals. This circumstance can be used for the study of the spin polarization of different electron groups of a ferromagnet, since two-quantum annihilation is possible only from the spin-singlet state of the annihilating pair.[66, 67]

The simplest method of investigating a ferromagnet with the aid of polarized positrons is to observe the difference between two angular-correlation curves corresponding to directions of magnetization parallel and antiparallel to the direction of the positron polarization. This effect was first observed by Hanna and Preston.[59] They have shown that for iron the quantity

$$A(\theta) = \int_\theta^\infty [N^+(\theta') - N^-(\theta')]\, d\theta'$$

is positive in the region of large angles θ, and increases with increasing θ. (The functions $N^\pm(\theta)$ are the angular distributions for two directions of the magnetic field relative to the direction of the positron polarization. The plus corresponds to parallel **H** and $\mathbf{s}_p$. A similar meaning is possessed also by the other physical quantities designated in the same manner.)

As follows from (3.4), the γ quantum pairs deflected through large angles θ are produced essentially as a result of annihilation of positrons with localized electrons. Thus, from the sign of the quantity $A(\theta)$ at large angles θ ($\theta > \theta_F$) it is possible to deduce the direction of the magnetization of these electrons relative to the total magnetization of the sample. From the results of the experiment of Hanna and Preston it follows that for iron the direction of the summary magnetic moment of the localized electrons (3d electrons) coincides with the direction of the magnetization of the sample.

An attractive possibility is to use experiments of this kind to investigate the spin polarization of weakly localized electrons. To this end, they investigated in [60–64] the quantity $n(\theta) = N^+(\theta) - N^-(\theta)$ for iron and nickel. The results obtained by Mijnarends and Hambro[60] with single-crystal iron are shown in Fig. 16. The crystal was so oriented that the momentum distribution was plotted relative to the [110] direction. In this case the quantity $N^+(\theta) - N^-(\theta)$ reverses sign at $\theta \simeq \theta_F$. However, it is in general impossible to conclude that this circumstance is connected with the negative polarization of the 4s electrons relative to the 3d electrons.[62] Indeed, if we neglect the probability of three-quantum annihilation compared with two-quantum annihilation, then for any spin configuration of the 4s and 3d electrons there should be satisfied the equality

$$\int_{-\infty}^{\infty} N^+(\theta)\, d\theta = \int_{-\infty}^{\infty} N^-(\theta)\, d\theta. \tag{5.1}$$

The validity of this expression follows from the fact that both terms in (5.1), depend, when 3γ-annihilation is neglected, only on the number of positrons entering into the sample and on the geometry of the setup, i.e., on

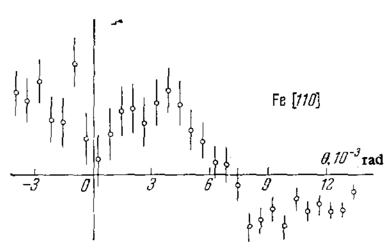

FIG. 16. Results obtained with single-crystal iron [60] for the quantity $n(\theta) = N^+(\theta) - N^-(\theta)$. The superscripts + and – indicate the direction of the magnetic field relative to the direction of the positron polarization (the ordinates represent $-n(\theta)$).

factors that do not depend on the direction of the magnetic field.

Thus, if $N^+(\theta) - N^-(\theta) > 0$ when $\theta > \theta_F$, then in the case of small θ, according to (5.1), $N^+(\theta) - N^-(\theta)$ should automatically reverse sign. If we take into consideration the possibility of three-quantum annihilation, then (5.1) no longer holds. However, the degree to which this equality is violated is quite small. Let us denote the right and left sides of (5.1) by $K_{2\gamma}^+$ and $K_{2\gamma}^-$; then, as shown in [62] (and will be discussed in detail later), we have for iron, when 3γ-annihilation cases are taken into account, $K_{2\gamma}^+ - K_{2\gamma}^-/K_{2\gamma}^\pm \sim 0.1\%$.

Thus, from the general behavior of the function $n(\theta)$ at large and small values of θ it is impossible to draw any conclusions concerning the polarization of the 4s electrons. It is possible, however, to obtain information concerning this quantity by investigating in detail, in single crystals, the detailed structure of the function $n(\theta)$. In principle, such a possibility is afforded by the fact that the Fermi surfaces are not the same for two 4s-subbands with different spin orientation, in the case when these electrons are polarized. The difference between the end-point momenta p_F^+ and p_F^- can leave certain "traces" on the curve describing the function $n(\theta)$. (The quantities p_F^+ and p_F^- describe respectively electrons with spin magnetic moment directions parallel and antiparallel to the direction of the magnetic field.)

Figure 17 shows plots of $n'(\theta) = [N^+(\theta) - N^-(\theta)]/[N^+(\theta) + N^-(\theta)]$ for single-crystal nickel oriented in the directions [100] and [111].[82] There is no doubt that the complicated structure of these curves contains much information on the band structure of nickel. However, a number of difficulties arise in the interpretation of these results. First of all, it is necessary to have for this purpose certain definite information concerning the topology of the Fermi surface of nickel, the properties of which have not been well investigated so far. In addition, the details of the curves shown in Fig. 17 depend on the concrete form of the electron wave functions. Finally, difficulties that arise in the interpretation of these curves become aggravated by the fact that these curves characterize the distributions of the electrons only with respect to one component of the momentum, and constitute the result of averaging of distributions over the two other momentum components. In view of the foregoing difficulties, which arise in the interpretation of the experimental data for $n(\theta)$, the authors of [82] were unable to draw any definite conclusions concerning the band structure of nickel on the basis of the curves shown in Fig. 17.

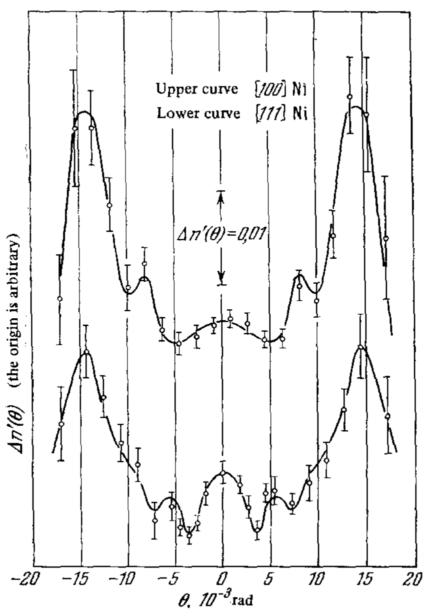

FIG. 17. Results obtained for the quantity $n'(\theta) = [N^+(\theta) - N^-(\theta)]/[N^+(\theta) + N^-(\theta)]$ of single-crystal nickel [82]. The upper and lower curves correspond to crystal orientations at which the momentum distributions of the γ-quantum pairs were investigated respectively along the axes [100] and [111].

Certain conclusions concerning the polarization of weakly localized electrons can be drawn by measuring the difference between the total number of cases of two-quantum annihilations when the magnetic field is directed parallel and antiparallel to the positron polarization direction,[63] i.e., from the quantity $K_{2\gamma}^+ - K_{2\gamma}^-$. To this end, let us consider the expression for the ratio of the cases of 2γ and 3γ annihilations $(K_{2\gamma}/K_{3\gamma})^+$ and $(K_{2\gamma}/K_{3\gamma})^-$ corresponding to the two magnetic-field directions.

As already noted in Ch. II, the 2γ annihilation can take place only from the spin-singlet state, whereas the 3γ annihilation can take place from the spin-triplet state. In the case when the polarized positron is in a ferromagnetic metal, the probabilities of the spin-singlet and spin-triplet overlaps of the wave functions of the positron and the electrons, namely the values κ_1 and κ_2 respectively, are equal to

$$\varkappa_1 = \frac{1}{4}\sum_j (1 - P_e^j P_p^0) w_j, \quad \varkappa_2 = \frac{1}{4}\sum_i (3 + P_e^i P_p^0) w_i. \tag{5.2}$$

In these expressions, the summation is over all the occupied electron states; P_e^i is the polarization of the electron in the i-th state; P_p^0 is the polarization of the thermalized positron ($-1 \le P_{e,p} \le 1$); w_i is the interval of the overlap of the wave functions of these particles, i.e.,

$$w_i = \int |\Psi_{i,e}(\mathbf{x})\Psi_{0,p}(\mathbf{x})|^2 d^3\mathbf{x}. \tag{5.3}$$

It follows from (5.2)[62] that

$$\left(\frac{K_{2\gamma}}{K_{3\gamma}}\right)^{\pm} = \frac{3\sigma_{2\gamma}}{\sigma_{3\gamma}} \frac{\sum_i (1 \mp P_e^i P_p^0) w_i}{\sum_j (3 \pm P_e^j P_p^0) w_j}. \tag{5.4}$$

Here $\sigma_{2\gamma}$ and $\sigma_{3\gamma}$ are the cross sections of two- and three-quantum annihilations; $\sigma_{2\gamma}/\sigma_{3\gamma} = 372$.[71] Besides expression (5.4), the quantities $K_{2\gamma}^\pm$ and $K_{3\gamma}^\pm$ are connected by the equality

$$K_{2\gamma}^+ + K_{3\gamma}^+ = K_{2\gamma}^- + K_{3\gamma}^-. \tag{5.5}$$

Let us denote $(K_{2\gamma}^+ - K_{2\gamma}^-)/K_{2\gamma}^-$ by λ, and the right sides of (5.4) by $f^\pm$. With the aid of simple derivations we can obtain from (5.4) and (5.5) the expression

$$\left(1 + \frac{1}{f^+}\right)\lambda = \frac{1}{f^-} - \frac{1}{f^+}, \tag{5.6}$$

or, since $f^\pm \sim 3\sigma_{2\gamma}/\sigma_{3\gamma} \sim 10^3$,

$$\lambda \simeq \frac{1}{f^-} - \frac{1}{f^+}. \tag{5.7}$$

Thus, if the parameters λ, P_p, and w_i are known, then the relation (5.6) can be used in metal research as a certain additional condition relating the values of the spin polarizations of different electron groups.

VI. ANNIHILATION WITH PRODUCTION OF n PHOTONS

An isolated electron–positron pair can decay only into two or more γ quanta. Single-quantum annihilation for such a pair is forbidden by the energy and momentum conservation laws. Thus, in this case the most probable process is two-quantum annihilation. The probability of annihilation with emission of n photons decreases rapidly with increasing n, since $W_{(n+1)\gamma}/W_{n\gamma}$ is determined, in order of magnitude, by the fine-structure constant.

An electron–positron pair annihilating in a solid is not free. In this connection, cases of single-quantum or even no-quantum annihilation are possible (in the latter case a fast electron may be emitted). The probabilities of such processes differ in practice from zero only in the case of interaction of fast positrons with electrons of the internal shells that are closest to the nucleus. Therefore the fraction of positrons participating in such effects is small compared with the total number of positrons falling into the solid. According to estimates,[68, 69] the ratio of the numbers corresponding to the cases of one-quantum and two-quantum annihilation in lead is approximately 0.2% if a typical radioactive source is used. The analogous ratio for the cases of no-quantum and two-quantum annihilation is 0.0015%. At the present time, neither of the effects noted above has found application for the investigation of the properties of solids.

Effects connected with three-quantum annihilation in metals have so far been investigated in much less detail than effects of two-quantum annihilation. Experiments performed in this field have been devoted essentially to a determination of the ratio of the cases of 3γ and 2γ annihilation. From the calculations of Ore and Powell[71] it follows that the ratio of the cross sections of 3γ and 2γ annihilation for three unpolarized particles with small relative velocities is $1/372$. In those cases when the annihilation occurs from bound states in vacuum, the ratio of the cases of 3γ and 2γ annihilation is equal to the ratio of the number of atoms of ortho- and para-positronium. If the positronium is produced in matter, then the number of cases of three-quantum annihilation is no longer determined simply by the amount of ortho-positronium, since the annihilation can take place as the result of capture of an electron from the surrounding medium by a positron which is in the bound state. In this case, the existence of ortho-positronium leads only to a certain additional contribution to the total number of cases of three-quantum annihilation. For dielectrics in which positronium is produced, the magnitude of this contribution is of the order of 10^{-2} (see, e.g.,[72, 73]

As already noted in Ch. II, in some metals there is a weakly pronounced long-lived lifetime component. This circumstance has induced many authors[74-78] to investigate the ratio of the cases of two- and three-quantum annihilations in metals. Absolute measurements of this ratio in aluminum were made by De Benedetti and Siegel[76] and also by Basson.[77] According to Basson's results, this ratio is equal to 402 ± 50. Such a result does not contradict the theoretical conclusions of Ore and Powell.

In the remaining studies of this question, they investigated not the absolute value of $W_{3\gamma}/W_{2\gamma}$, but only the difference between these quantities for different metals. According to the results of [78], $W_{3\gamma}/W_{2\gamma}$ does not remain constant for different metals. If these ratios are compared with those corresponding to aluminum, then the maximum deviations, approximately 15%, takes place for nickel, platinum, and lead. According to authors of that paper, there is no second lifetime component for these metals. Thus, this effect has no definite interpretation at present.

In conclusion, it should be noted that the number of presently published papers devoted to annihilation of positrons in condensed bodies increases rapidly. At the same time, the number of questions whose study is made possible with the aid of effects accompanying positron annihilation also increases rapidly.

[1] G. Lee-Whiting, Phys. Rev. 97, 1557 (1955).

[2] V. I. Karpman and I. Z. Fisher, Dokl. Akad. Nauk SSSR 111, 1212 (1956) [Sov. Phys.-Dokl. 1, 765 (1957)].

[3] R. Ferrell, Rev. Mod. Phys. 28, 308 (1956).

[4] A. Held and S. Kahana, Canad. J. Phys. 42, 1908 (1964).

[5] H. Kanarawa, J. Ohtsuki, and S. Janagawa, Phys. Rev. A138, 1155 (1965).

[6] S. De Benedetti and H. Richings, Phys. Rev. 85, 377 (1952).

[7] A. Ferguson and G. Lewis, Phil. Mag. 44, 1338 (1953).

[8] R. Bell and R. Graham, Phys. Rev. 90, 644 (1953).

[9] G. Minton, Phys. Rev. 94, 758 (1954).

[10] I. Gerholm, Ark. Fys. 10, 523 (1956).

[11] H. Weisberg, Bull. Am. Phys. Soc. 10, 21 (1965).

[12] R. Bell and M. Jørgensen, Canad. J. Phys. 38, 652 (1960).

[13] A. Bissi, G. Faini, E. Gatti, and L. Zappa, Phys. Rev. Lett. 5, 59 (1960).

[14] G. Jones and J. Warren, Canad. J. Phys. 39, 1517 (1961).

[15] J. Rodda and M. Stewart, Phys. Rev. 131, 255 (1963).

[16] S. De Benedetti, Nuovo cimento 4, Suppl. No. 3, 1209 (1956).

[17] A. I. Akhiezer and V. B. Berestetskiĭ, Kvantovaya elektrodinamika, Fizmatgiz, 1959 [Quantum Electrodynamics, Interscience, 1965].

[18] S. Kahana, Phys. Rev. 129, 1622 (1963).

[19] E. Jackson and J. McGervey, Bull. Am. Phys. Soc. 9, 686 (1964).

[20] N. March and A. Murray, Phys. Rev. 126, 1480 (1962).

[21] A. Zuchell and T. Hickmann, Phys. Rev. A136, 1728 (1966).

[22] V. L. Sedov, Fiz. Tverd. Tela 9, 1957 (1967) [Sov. Phys.-Solid State 9, 1540 (1968)].

[23] J. Du Mond, D. Lind, and B. Watson, Phys. Rev. 75, 1226 (1949).

[24] N. A. Vlasov and B. S. Dzhelepov, Dokl. Akad. Nauk SSSR 70, 207 (1950).

[25] S. De Benedetti, C. Cowan, W. Konneker, and H. Primakoff, Phys. Rev. 77, 208 (1950).

[26] R. Green and A. Stewart, Phys. Rev. 98, 486 (1955).

[27] A. Stewart, Phys. Rev. 99, 594 (1955).
[28] G. Lang, S. De Benedetti, and R. Smoluchowski, Phys. Rev. 99, 596 (1955).
[29] G. Lang and N. Hien, Phys. Rev. 110, 1062 (1958).
[30] G. Lang and S. De Benedetti, Phys. Rev. 108, 914 (1957).
[31] K. A. Baskova and B. S. Dzhelepov, Izv. AN SSSR ser. fiz. 20, 951 (1956).
[32] A. Stewart, Canad. J. Phys. 35, 168 (1957).
[33] S. Berko and S. Plaskett, Phys. Rev. 112, 1877 (1958).
[34] G. Trumpy, Phys. Rev. 118, 668 (1960).
[35] I. Ya. Dekhtyar and V. S. Mikhalenkov, Dokl. Akad. Nauk SSSR 133, 60 (1960) [Sov. Phys.-Dokl. 5, 739 (1961)].
[36] I. Ya. Dekhtyar and V. S. Mikhalenkov, ibid. 136, 63 (1961) [6, 31 (1961)].
[37] I. Ya. Dekhtyar, S. G. Litovchenko, and V. S. Mikhalenkov, ibid. 147, 1332 (1962) [7, 1135 (1963)].
[38] S. Berko, Phys. Rev. 128, 2166 (1962).
[39] A. Stewart, Phys. Rev. 123, 1587 (1961).
[40] V. L. Sedov, Zh. Eksp. Teor. Fiz. 45, 2070 (1963) [Sov. Phys.-JETP 18, 1419 (1964)].
[41] J. Donaghy and A. Stewart, Bull. Am. Phys. Soc. 9, 238 (1964).
[42] K. Fujiwara, J. Phys. Soc. Japan 20, 1533 (1965).
[43] R. Williams, T. Loucks, and A. Mackintosh, Phys. Rev. Lett. 16, 168 (1966).
[44] K. Fujiwara and O. Sueoka, J. Phys. Soc. Japan 21, 1947 (1966).
[45] A. Stewart and N. Pope, Phys. Rev. 120, 2033 (1960).
[46] A. Stewart, J. Shand, J. Donaghy, and J. Kusmiss, Phys. Rev. 128, 118 (1962).
[47] A. Stewart, J. Kusmiss, and K. March, Phys. Rev. 132, 495 (1963).
[48] D. Gustafson and A. Mackintosh, J. Phys. Chem. Solids 25, 389 (1964).
[49] L. Page and M. Heinberg, Phys. Rev. 102, 1545 (1956).
[50] R. De Zafra and W. Joyner, Phys. Rev. 112, 19 (1958).
[51] I. Ya. Dikhtyar, D. A. Levina, and V. S. Mikhalenkov, Dokl. Akad. Nauk SSSR 156, 795 (1964) [Sov. Phys.-Dokl. 9, 492 (1964)].
[52] I. Ya. Dikhtyar, V. S. Mikhalenkov, and S. G. Sakharova, ibid. 168, 785 (1966) [11, 537 (1966)].
[53] M. A. Krivoglaz and A. A. Smirnov, FMM 7, 151 (1959).
[54] J. Carbotte and S. Kahana, Phys. Rev. A139, 213 (1965).
[55] A. Stewart and J. Shand, Phys. Rev. Lett. 16, 261 (1966).
[56] C. Majumdar, Phys. Rev. 149, 406 (1966).
[57] C. Majumdar, Phys. Rev. A140, 237 (1965).
[58] D. Hamann, Phys. Rev. 146, 277 (1966).
[59] S. Hanna and R. Preston, Phys. Rev. 109, 716 (1958).
[60] P. Mijnarends and L. Hambro, Phys. Lett. 10, 272 (1964).
[61] J. Lovas, Nucl. Phys. 17, 279 (1960).
[62] S. Berko and J. Zuckerman, Phys. Rev. Lett. 13, 339 (1964).
[63] V. L. Sedov, Zh. Eksp. Teor. Fiz. 48, 1200 (1965) [Sov. Phys.-JETP 21, 800 (1965)].
[64] T. Mihalisin and R. Parks, Phys. Lett. 21, 610 (1966).
[65] P. Wallace, Solid State Physics 10, 1 (1960).
[66] J. Phillips, Phys. Rev. A133, 1020 (1964).
[67] H. Ehrenreich, J. Phillips, and D. Olechna, Phys. Rev. 131, 2469 (1964).
[68] J. Jaeger and H. Hulme, Proc. Cambr. Phil. Soc. 32, 158 (1936).
[69] L. Sodickson, W. Bowman, and J. Stephenson, Phys. Rev. 124, 1851 (1961).
[70] S. Shimizu, T. Mukoyama, and Y. Nakayama, Phys. Lett. 17, 295 (1965).
[71] A. Ore and J. Powell, Phys. Rev. 75, 1696 (1949).
[72] R. Graham and A. Stewart, Canad. J. Phys. 32, 678 (1954).
[73] A. Gainotti, E. Germagnolli, G. Schianchi, and L. Zecchina, Nuovo cimento 32, 880 (1964).
[74] S. De Benedetti and R. Siegel, Phys. Rev. 85, 371 (1952).
[75] T. Pond, Phys. Rev. 93, 479 (1954).
[76] S. De Benedetti and R. Siegel, Phys. Rev. 94, 956 (1954).
[77] J. Basson, Phys. Rev. 96, 691 (1954).
[78] M. Bertolaccini, C. Bussolati, and L. Zappa, Phys. Rev. A139, 696 (1965).
[79] V. I. Gol'danskiĭ and E. P. Prokop'ev, ZhETF Pis. Red. 4, 422 (1966) [JETP Lett. 4, 284 (1966)].
[80] A. Dafner and A. Bushkovitch, Bull. Am. Phys. Soc. 9, 562 (1964).
[81] D. A. Kirzhnits, Polevye metody teorii mnogikh chastits (Field Methods of Many-particle Theory), Gosatomizdat, 1963.
[82] T. Mihalisin and R. Parks, Phys. Rev. Lett. 18, 210 (1967).

Translated by J. G. Adashko